Journal of Zhejiang University SCIENCE A
ISSN 1673-565X (Print); ISSN 1862-1775 (Online)
www.zju.edu.cn/jzus; www.springerlink.com
E-mail: jzus@zju.edu.cn

Development of an ε-type actuator for enhancing high-speed electro-pneumatic ejector valve performance*

Zhong XIANG†, Hao LIU†‡, Guo-Liang TAO, Jun MAN, Wei ZHONG

(*State Key Laboratory of Fluid Power Transmission and Control, Zhejiang University, Hangzhou 310027, China*)

†E-mail: zju_xiang@hotmail.com; hliu2000@zju.edu.cn

Received May 6, 2008; revision accepted Aug. 25, 2008

Abstract: A novel ε-type solenoid actuator is proposed to improve the dynamic response of electro-pneumatic ejector valves by reducing moving mass weight. A finite element analysis (FEA) model has been developed to describe the static and dynamic operations of the valves. Compared with a conventional E-type actuator, the proposed ε-type actuator reduced the moving mass weight by almost 65% without significant loss of solenoid force, and reduced the response time (RT) typically by 20%. Prototype valves were designed and fabricated based on the proposed ε-type actuator model. An experimental setup was also established to investigate the dynamic characteristics of valves. The experimental results of the dynamics of valves agreed well with simulations, indicating the validity of the FEA model.

Key words: ε-type actuator, High-speed electro-pneumatic ejector valve, Finite element method, Dynamic simulation and experiment

doi:10.1631/jzus.A0820350 **Document code:** A **CLC number:** TM15; TH138

INTRODUCTION

With advantages of low cost, anti-pollution ability, high flow rate gain, small size and simple structure (Topçu *et al*., 2006; Khan *et al*., 2007), high-speed electro-pneumatic ejector valves have attracted considerable attention in several areas of modern industry. They have been used in sorting parts, flapping control systems and other systems for gluing, dosing and packaging where discrete cyclic, linear or rotating motions and a very long lifetime are required. These modern high-speed electro-pneumatic valve applications need further improvements including higher operating speed, improved reproducibility of the opening and closing phase, and weight, volume and cost reduction (Ertl *et al*., 2003).

There have been many developments in fast response actuators over the past two decades. First, Seilly (1979; 1981) studied two kinds of solenoid actuators, called Helenoid and Colenoid. Further research then followed, aimed at improving the dynamic response of actuators by developing new kind of solenoids or improving the old ones. Schechter (1982) developed a kind of fast response multipole solenoid actuator with a 2-ms response time (RT). Kushida (1985) developed a disk type solenoid actuator (called DISOLE) with an RT of less than 1 ms. Recently, piezotranslators have also been developed for use as actuators of ejectors. Zhao and Jones (1991) developed a fast response electro-pneumatic power converter by combining a stacked piezotranslator flapper as a drive stage and a back pressure stage for generating the output. Lee (1999) designed fast actuators using multilayer stacked alkali halide electrostrictive materials for fuel injection. Although these proposed actuators have fairly good performances, they are not popular in the design of high-speed electro-pneumatic ejector valves because of their large size, high cost or complex structure. They are not well suited to some of the characteris-

‡ Corresponding author

* Project supported by the Doctoral Fund of Ministry of Education of China (No. 20070335133) and the Educational Commission of Zhejiang Province (No. 20070057), China

tics inherent in high-speed electro-pneumatic ejector valves, including small stroke length (0.05~0.10 mm) and low working pressure (less than 1.0×10^6 Pa). Neither are they well suited to the needs of industrial applications including small size, low cost, large force production, lack of operation maintenance under continuous duty cycles at 150~300 Hz and multibillion cycle operation (in excess of five billion cycles) (Khan *et al.*, 2007).

On the contrary, classical C-type and E-type actuators are still favored for use as ejector valve actuators because of their simplicity and high holding force capability. For example, Fig.1 shows a schematic cross section through a typical actuator that has been used in an ejector valve. The symbols (e.g., l_g, d_{in}) used in Fig.1 and Fig.2 (see in next section) for dimensional parameters normally consist of a prefix character, l for length and d for diameter, and a subscript to differentiate from each other. It is obvious that the actuator showed in Fig.1 is essentially an E-type actuator that consists of an excitation coil wound around a magnetic E-core stator and a disk steel armature (moving mass). The armature will be caught or released by energizing or de-energizing the wound coil. The solenoid force produced by the actuator is needed to overcome the reaction force to which the armature is subjected as a result of high-pressure air flowing through the valve. As proved by Schechter (1982) and Seilly (1979; 1981), with an E-type (or C-type) actuator, the larger the solenoid force required, the lower the acceleration of the armature (moving mass). This presents a substantial challenge to obtaining further improvement in the valve dynamics within its compact packaging size.

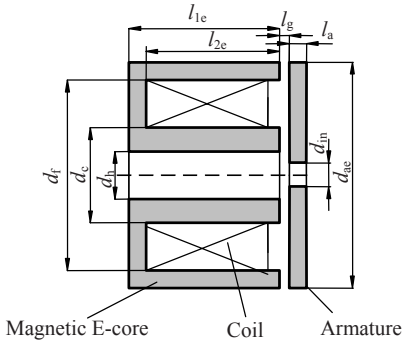

Fig.1 Definitions of dimensional parameters for a conventional E-core stator and disk armature

This paper describes the development of an ε-type actuator (in cross section, the shape of the actuator looks like the character ε) to balance the increased solenoid force and the decreased armature acceleration inherent in E-type actuators to enhance the performance of electro-pneumatic ejector valves. The finite element analysis (FEA) method is used to model and simulate the actuator and the fabricated ejector valve. Steady state and dynamic response characteristics of E-type and ε-type actuators are thoroughly compared. Finally, simulated dynamic displacement and current results of the actuator are contrasted with the experimental results, respectively. As an example of application, the newly developed high-speed pneumatic ejector valves are used in the ejection systems of high-speed optical food sorting machines.

FINIT ELEMENT ANALYSIS MODELLING

Description of the ε-type actuator and design of the prototype valve

Fig.2a illustrates the schematic structure of the proposed ε-type actuator. Compared with the E-type actuator (Fig.1), a 'core shoulder' is introduced into the ε-type actuator structure. The structural dimensions of both actuators are almost the same while the armature (moving mass) weight of the ε-type actuator is reduced considerably. As proved below, the solenoid force produced by an ε-type actuator is almost the same as that produced by an E-type actuator, but the dynamic response performance of the ε-type actuator is much improved.

Fig.2b shows a schematic cross section of the fabricated prototype valve. The valve can be divided into three major bodies (bodies I, II, III). Body I consists of a magnetic ε-core, a wound coil and a plastic ring, and provides an air inlet port. A wire tunnel is also drilled in it. Body II has a circular chamber in the center to house the armature. The diameter of the chamber is designed to be slightly bigger than that of the armature to ensure that the armature can move freely. Four semicircular slots are distributed evenly along the inner circumference of body II to improve the flow rate of the valve. Body III provides an air outlet port, shown in detail in Fig.2c (top view). The coil consists of 150 turns of

isolated copper wire with a resistance of 3.2 Ω. It is directly wound on the magnetic core to improve the heat-sinking capacity of the valve. All three bodies are made of hard aluminum and are joined together with four hexagonal socket countersunk head screws. The valve is sealed with O-rings or rubber sheet. Contact faces, such as the lower face of the armature and the upper face of body III, are abrasively trimmed to ensure accurate assembly and provide a good seal. The height of the magnetic core is designed to be typically 0.05 mm less than that of the magnetic frame to reduce the close contact area between the armature upper face and the actuator core. Grooves are also milled in the lower face of the magnetic frame so that the armature can return as soon as the coil is de-energized.

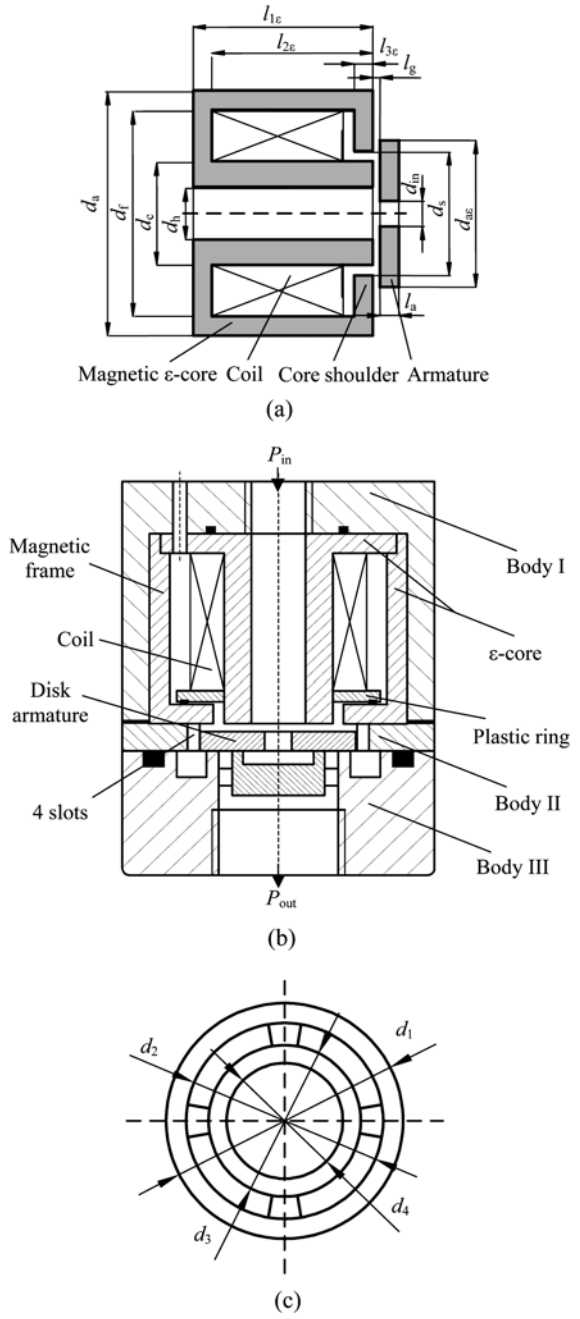

Fig.2 Definitions of dimensional parameters for (a) the proposed ε-core stator and disk armature, (b) schematic cross section of the prototype valve and (c) top view of the body III

For all of the following numerical simulations and experiments, Table 1 lists all the actuator dimensional parameters (for detail please refer to Fig.1 and Fig.2a) and Table 2 lists all other parameters adopted unless otherwise stated. Fig.3 shows the magnetization characteristics of the material used for both type actuators' armature and stator core.

Table 1 Specification of the E-type and ε-type actuators

Dimension (mm)	E-core and armature	ε-core and armature
d_h	4	4
d_c	8	8
d_f	16	16
l_a	1.5	1.5
d_a		19
d_{ae}	19	
d_{in}	3.6	3.6
$d_{a\varepsilon}$		11.4
l_{1e}	13	
$l_{1\varepsilon}$		13.9
l_{2e}	11.5	
$l_{2\varepsilon}$		12.4
$l_{3\varepsilon}$		0.9
d_1		10.6
d_2		8.8
d_3		6.8
d_4		5.2
d_s		10

Table 2 Data for modeling the system

Parameter	Value
Electric permittivity of free space ξ_0 (F/m)	8.85×10^{-12}
Actuator material electrical conductivity σ (S/m)	1×10^{6}
Coil resistance R (Ω)	3.2
Density of the material ρ (kg/m^3)	7.65×10^{3}
Damping coefficient of air b (N·s/m)	1.8×10^{-5}
Absolute ambient pressure P_a (N/m^2)	1.01×10^{5}

Electromagnetic field sub-model

2D axisymmetric FEA models can be built to

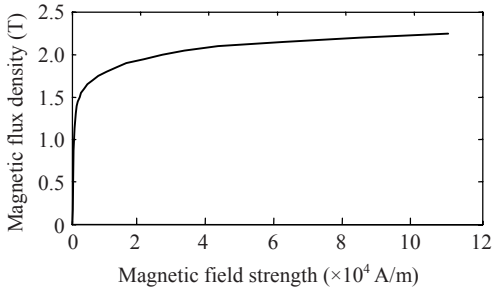

Fig.3 Initial magnetization curve for E-type and ε-type actuators

simulate both actuators (Figs.1 and 2). Assuming that the material used for the actuator is isotropic and its hysteresis can be neglected, electromagnetic fields are governed by Maxwell equations (Eqs.(1)~(4)) with displacement currents ignored (quasi stationary limit) while the constitutive equation is expressed as Eq.(5) (Nannapaneni, 2004):

$$\nabla \times \boldsymbol{H}(r,t) = \boldsymbol{J}(r,t), \tag{1}$$

$$\nabla \cdot \boldsymbol{B}(r,t) = 0, \tag{2}$$

$$\nabla \times \boldsymbol{E}(r,t) = -\frac{\partial \boldsymbol{B}(r,t)}{\partial t}, \tag{3}$$

$$\nabla \cdot \boldsymbol{E}(r,t) = \frac{\rho(r,t)}{\xi_0}, \tag{4}$$

$$\boldsymbol{H} = v\boldsymbol{B}, \quad \boldsymbol{J} = \sigma \boldsymbol{E}, \tag{5}$$

where $\boldsymbol{H}$ is the magnetic-field intensity, r is the radial coordinate in the cylindrical coordinate system, $\boldsymbol{B}$ is the magnetic flux density, $\boldsymbol{J}$ is the current density, $\boldsymbol{E}$ is the electric-field intensity, ρ is the volumetric charge density, ξ_0 is the electric permittivity of free space, v is the material reluctivity, and σ is the electrical conductivity.

By introducing magnetic vector potential $\boldsymbol{A}$ and electrical scalar potential φ, and combining with Coulomb gauge condition and Dirichlet boundary condition, Maxwell equations can be expressed as (Pawlak and Nehl, 1988; Khan *et al.*, 2007):

$$\boldsymbol{B} = \nabla \times \boldsymbol{A}, \tag{6}$$

$$\nabla \cdot \left(\frac{\partial \boldsymbol{A}}{\partial t} - \nabla \varphi \right) = 0, \tag{7}$$

$$\nabla \times (v \nabla \times \boldsymbol{A}) = \boldsymbol{J} - \sigma \frac{\partial \boldsymbol{A}}{\partial t} + \frac{\mathrm{d}\delta}{\mathrm{d}t} \sigma \times (\nabla \times \boldsymbol{A}), \tag{8}$$

where δ is the armature displacement.

In the transient case with motion, an additional circuit equation should be simultaneously solved with the partial differential equation of the magnetic field. The following voltage equation is used to couple the electric and magnetic models:

$$U(t) = IR + L(\delta, I)\frac{\mathrm{d}I}{\mathrm{d}t} + I\frac{\mathrm{d}\delta}{\mathrm{d}t}\frac{\partial L(\delta, I)}{\partial x}, \tag{9}$$

where U, I, R, L are the external energizing voltage, coil current, coil resistance and wound coil reluctance, respectively.

The total solenoid force F_{mag} produced by the actuator can be derived by integrating the Maxwell stress tensor $\boldsymbol{T}$ over the surface S surrounding the armature as Eq.(10):

$$F_{\mathrm{mag}} = \oint_S \boldsymbol{T}\boldsymbol{n}\mathrm{d}S. \tag{10}$$

Mechanical sub-model

Taking solenoid force, moving mass, viscous damping and pressure force into account and applying Newton's 2nd law, the governing equation for the armature can be expressed as

$$F_{\mathrm{mag}} = m\left(\frac{\mathrm{d}^2\delta(t)}{\mathrm{d}t^2} + g\right) + b\frac{\mathrm{d}\delta(t)}{\mathrm{d}t} + F_{\mathrm{p}}, \tag{11}$$

$$m = \rho_{\mathrm{m}} V, \tag{12}$$

where g is the gravity, b is the viscous damping coefficient of the air, F_{p} is the pressure force acting on the armature, and m, ρ_{m} and V are the mass, material density and volume of the armature, respectively.

Referring to Fig.2b and Fig.2c, Eq.(13) can be used to estimate the static pressure force, F_{sp}, acting on the armature when it is released by the magnetic core (closed state):

$$\frac{\pi}{4}(d_2^2 - d_3^2)(P_{\mathrm{s}} - P_{\mathrm{a}}) \le F_{\mathrm{sp}} \le \frac{\pi}{4}(d_1^2 - d_4^2)(P_{\mathrm{s}} - P_{\mathrm{a}}), \tag{13}$$

where P_{s} and P_{a} are the pressures at the valve inlet and outlet ports, respectively.

The flow status at the time when the armature is caught with the magnetic core (Fig.4) takes into account that there are grooves in the lower surface of the

magnetic frame and that the height of the magnetic core is a little less than that of the frame. Following Karidis and Turns (1982), we assumed that even when the valve was fully opened, there was still some clearance (about 0.01~0.02 mm) between the upper face of the armature and the lower face of the magnetic core shoulder. Owing to the fact that the clearance has the same magnitude as the small air gap length (0.05~0.10 mm), it can be assumed that the flow status during the armature movement (moving state) was the same as that when the armature was caught by the magnetic core (opened state). Therefore, the governing equation for static pressure force acting on the armature at the opened state has the same expression as that used for the dynamic pressure force acting on the armature. This pressure force can be obtained from the Navier-Stokes equations as

$$F_{\mathrm{dp}} = \frac{\pi(d_3^2 - d_4^2)}{4\ln(1 + d_4 / d_3)}(P_{\mathrm{s}} - P_{\mathrm{a}}). \qquad (14)$$

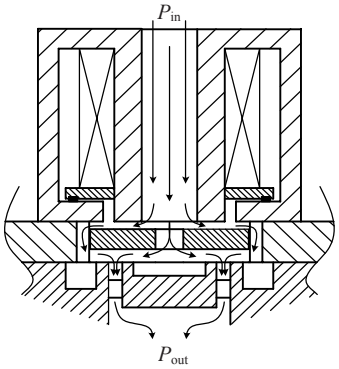

Fig.4 Flow status when valve is fully opened

SIMULATION AND EXPERIMENTAL ANALYSIS

Static simulation and comparison

For the steady-state force, constant current was adopted to excite the coil. The simulated static force-displacement and armature acceleration-displacement characteristics of the two actuators are plotted in Fig.5 as lines of constant magnetomotive force (MMF) values up to 1000 A (magnetic saturation). The accelerations were obtained by dividing the simulated solenoid forces by armature weight.

When the air gap length is small, the steady static solenoid forces produced by the ε-type actuator

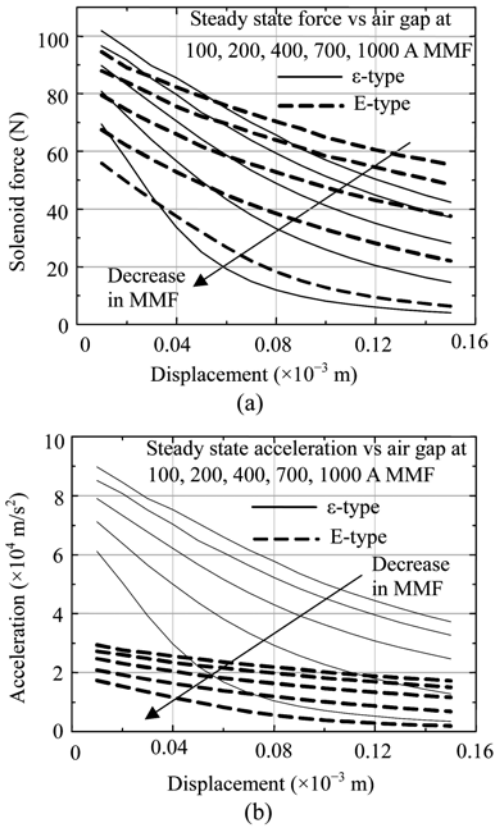

Fig.5 Simulated force-displacement (a) and acceleration-displacement (b) characteristics for the ε-type (solid lines) and E-type (dashed lines) actuators described in Table 1

are larger than those produced by the E-type actuator (Fig.5a). However, as the air gap length increases, the steady static solenoid forces produced by the ε-type actuator tend to be lower. Actuators for ejector valves typically operate at saturation conditions and their stroke lengths are less than 0.1 mm (Khan *et al*., 2007). The steady static solenoid forces of both actuators are almost the same in these situations (Fig.5a). Because the armature weight is considerably reduced by the ε-type actuator (by 65% here), the steady state armature acceleration of the ε-type actuator is obviously larger than that of the E-type actuator. For example, when the air gap has a typical length of 0.08 mm and under an excitation of 1000 A, the solenoid force and armature acceleration produced by the ε-type actuator are 66 N and 5.8×10^4 m/s^2, compared with those of 70 N and 2.2×10^4 m/s^2, produced by the E-type actuator, respectively. This feature of the ε-type actuator will enable it to respond faster than the E-type actuator.

Experimental setup

As the actuator stroke length is typically in the range of 0.05 ~0.10 mm, it is difficult and expensive to establish an experimental setup to accurately obtain the actuator force-displacement characteristics. Therefore, only a dynamic measurement setup was manufactured to validate the FEA model. Fig.6a shows the experimental setup used to detect the prototype valve dynamics. A laser sensor placed at its reference distance (150 mm) is used to detect the displacement of the armature. The hole in the bottom face of body III is turned large enough to ensure that the laser emitting from the sensor can pass through it and through the ventilated hole freely. Different work conditions can be easily realized by adjusting the regulator and the adjustable power supply. To avoid overheating the coil, a sophisticated energizing method (Seilly, 1979), integrated in the amplifier circuit (Fig.6b), is adopted to control the prototype valve. An adjustable parameter 10-kHz pulse width modulation (PWM) signal generated by NI/PCI-6251 multi-functional acquisition card is used to switch the power electronics.

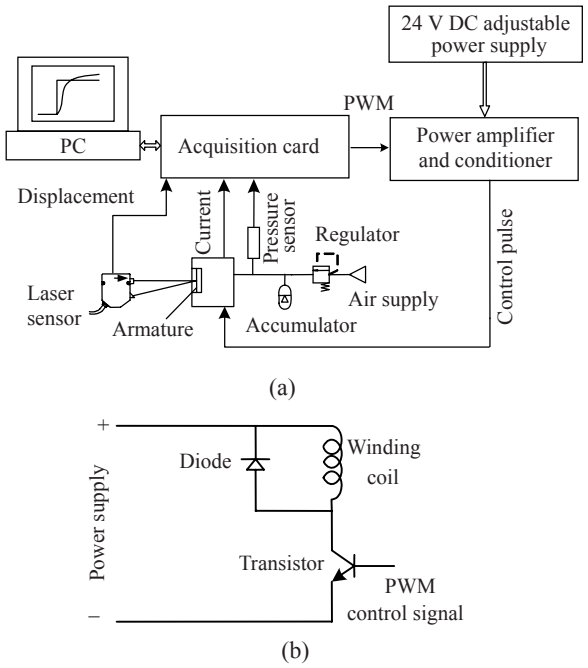

Fig.6 Experimental setup (a) and driving circuit (b) for prototype valve dynamics

Dynamic simulation and experiment

The dynamic characteristics of the ε-type actuator and the E-type actuator were compared with simulation results. For ease of comparison, constant exciting voltage is applied to the coil directly without any control strategy to make sure that the armature can be caught by the magnetic core. Initial conditions such as preload force, damping coefficient, etc., were all set to be the same for each actuator. The clearance between the contacted face of the armature and the magnetic core was experimentally set to 0.015 mm.

Fig.7 shows typical simulated sets of displacement curves for an ε-type actuator (solid lines) and a conventional E-type actuator (dashed lines). In particular, Fig.7a compares the effect of air gap length on the actuator movement when uniform exciting voltage (24 V) and preload force (13 N) are applied to both actuators. It clearly shows that the proposed ε-type actuator responds faster to the exciting signal than the E-type actuator. Quantitatively, RTs of the ε-type actuator at air gap lengths of 0.05 mm, 0.08 mm and 0.1 mm are decreased by 22%, 12% and 11%, respectively. Fig.7b compares the effect of external exciting voltage on the actuator movement when the same preload force is applied to both actuators. RTs of the ε-type actuator under exciting voltages of 24 V, 18 V and 12 V at 0.05 mm air gap length are decreased by 19%, 18% and 19%, respectively. Fig.7c compares the effect of preload force on the actuator movement when a uniform exciting voltage (24 V) is applied to both actuators. RTs of the ε-type under preload forces of 13 N, 20 N and 30 N at 0.05 mm air gap length are decreased by 20%, 19% and 22%, respectively.

Fig.8 shows the simulated (dashed lines) and experimental (solid lines) results of coil current and armature displacement for two fabricated prototype valves. The prototype valve in Fig.8a has an air gap length of 0.05 mm. It is excited by a 24 V, 0.3 ms pulse and operates under a pressure of 2.5×10^5 N/m^2 (static pressure force is about 13 N). The prototype valve in Fig.8b has an air gap length of 0.07 mm and is excited by a 24 V, 0.8 ms pulse and operates under a pressure of 3.5×10^5 N/m^2 (static pressure force is about 20 N). The oscillatory response of the experimental displacement curves occurring at the end of the armature movements (caught or released by the magnetic core) is caused by the frontal collisions between the armature and the magnetic core (or body III). This feature helps the valve open (or close) quickly when operating at high speed. The simulation results show a good agreement with the experimental results.

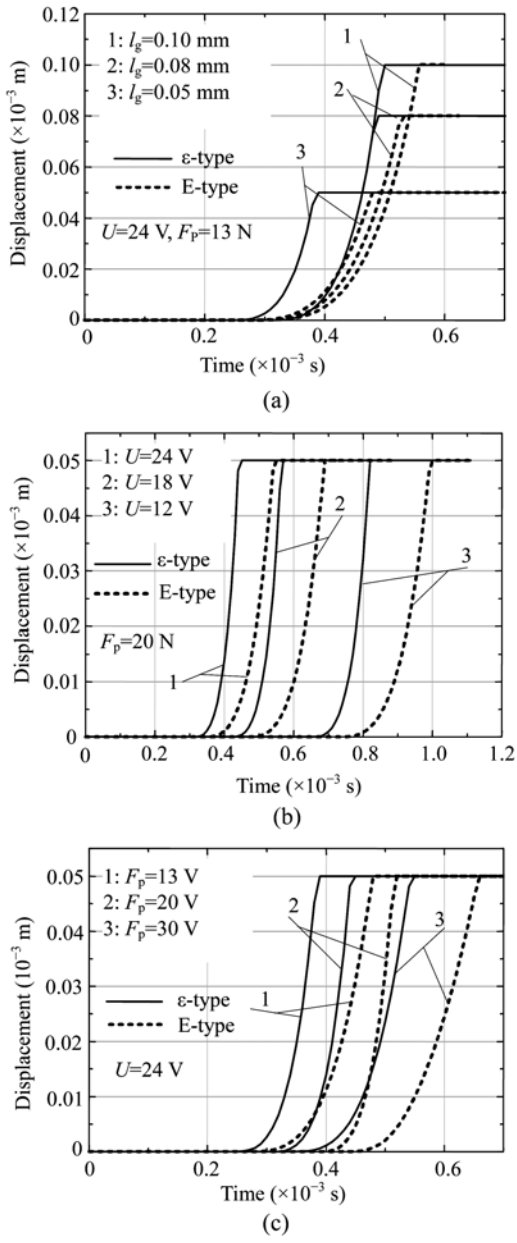

Fig.7 Simulated displacement curves for an ε-type actuator and an E-type actuator used for comparing the effects of air gap length (a), external exciting voltage (b) and preload force (c) on actuator dynamics

CONCLUSION

Balancing increasing solenoid force and decreasing armature acceleration is a critical problem in improving the dynamic response of high-speed electro-pneumatic valves. In this paper, we have proposed a solution to this problem by developing an ε-type actuator. Simulation results showed that the proposed ε-type actuator achieved a reduction of almost 65% in moving mass weight without a significant loss of steady state solenoid force in the actuator. This enabled the ε-type actuator to respond much faster than the conventional E-type actuator. In particular, it showed a 20% decrease in the RT to the external exciting signal under different work conditions. Experimental results from prototype valves validated the results of the simulations. The principle of the proposed ε-type actuator represents a new approach to further optimization of the design of high-speed electro-pneumatic ejector valves.

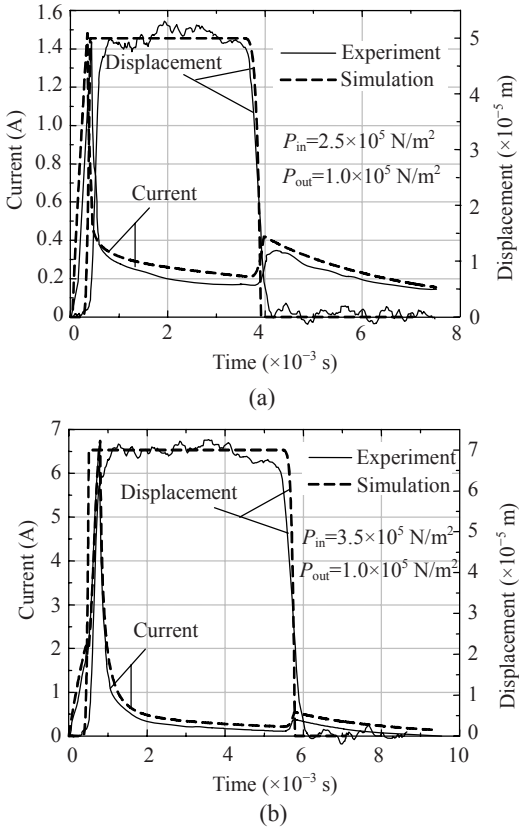

Fig.8 Simulated and experimental results of coil current and armature displacement response following (a) a 24 V, 0.3 ms pulse with a 0.05 mm air gap length and (b) a 24 V, 0.8 ms pulse with a 0.07 mm air gap length under different work conditions

References

Ertl, M., Kaltenbacher, M., Mock, R., Lerch, R., 2003. Numerical analysis of fast switching electromagnetic valves. *The International Journal for Computation and Mathematics in Electrical and Electronic Engineering*,

22(3):715-729. [doi:10.1108/03321640310475146]

Karidis, J.P., Turns, S.R., 1982. Fast-acting Electromagnetic Actuators—Computer Model Development and Verification. SAE Technical Papers Series, No. 820202, p.831-845.

Khan, S.H., Cai, M., Grattan, K.T.V, Kajan, K., Honeywood, M., Mills, S., 2007. Computation of 3-D magnetic field distribution in long-lifetime electromagnetic actuators. *IEEE Transaction on Magnetics*, **43**(4):1161-1164. [doi:10.1109/TMAG.2007.892277]

Kushida, T., 1985. High Speed Powerful and Simple Solenoid Actuator "DISOLE" and Its Dynamic Analysis Results. SAE Technical Papers Series, No. 850373, **3**:127-136.

Lee, F.S., 1999. Modeling of Actuator Systems Using Multilayer Electrostrictive Materials. Proceedings of the 1999 IEEE International Conference on Control Applications. Hawaii, USA, **2**:1406-1411. [doi:10.1109/CCA.1999.801178]

Nannapaneni, N.R., 2004. Elements of Engineering Electromagnetics. Prentice-Hall, Inc., Upper Saddle River, New Jersey.

Pawlak, A.M., Nehl, T.W., 1988. Transient finite element modeling of solenoid actuators: the coupled power electronics, mechanical, and magnetic field problem. *IEEE Transactions on Magnetics*, **24**(1):270-273. [doi:10.1109/20.43909]

Schechter, M.M., 1982. Fast Response Multipole Solenoids. SAE Technical Papers Series, No. 820203, p.846-857.

Seilly, A.H., 1979. Helenoid actuators—A New Concept in Extremely Fast Acting Solenoids. SAE Technical Papers Series, No. 790119, p.426-435.

Seilly, A.H., 1981. Colenoid Actuators—Further Developments in Extremely Fast Acting Solenoids. SAE Technical Papers Series, No. 810462, p.1440-1781.

Topçu, E.E., Yüksel, İ., Kamış, Z., 2006. Development of electro-pneumatic fast switching valve and investigation of its characteristics. *Mechatronics*, **16**(6):365-378. [doi:10.1016/j.mechatronics.2006.01.005]

Zhao, Y., Jones, B., 1991. A power air-jet actuator with piezotranslator drive stage. *Mechatronics*, **1**(2):231-243. [doi:10.1016/0957-4158(91)90045-C]